Examination of the powder spreading effect in Electron Beam Melting (EBM)

C. Eschey, S. Lutzmann, M. F. Zaeh

iwb Institute for Machine Tools and Industrial Management, Technische Universitaet Muenchen, Germany

Reviewed, accepted September 18, 2009

Abstract

In recent years, the scientific and industrial relevance of Electron Beam Melting (EBM) has grown. This is mainly due to the electron beam's extensive power density and flexible positioning properties. Thus, considerable building rates as well as a favorable part quality can be realized. However, the appearance of transient physical effects constitutes a substantial drawback towards the broader use of the technology. Therefore, experimental examinations are being carried out in order to investigate the effect of sudden powder spreading during beam material interaction. Based on an existing mathematical model, an analytical approach is formulated in order to implement effective counter measures. Hence, a significant increase in process stability is being achieved as the undesirable powder spreading effect is being avoided securely.

Introduction

Additive layer manufacturing is ideally suited to face current trends like increasing variety in versions at decreasing quantity. As the manufacture is done without a specific tool, the production of small batches can be conducted efficiently. The additive layer manufacturing for metal parts as well as for plastic parts is still dominated by systems using a laser beam source. Other technologies like electron beam melting still play only a negligible role. However, the use of an electron beam as an energy source for the selective melting of metal powder offers great potential like high beam spot velocity up to 5000 mm/s and beam power up to 10 kW. Therefore, it is subject of current research projects.

State of the art

Up to now, only a few research efforts have been conducted concerning the process modeling of EBM. These few focus on the structured coverage of influence coefficients by [1] and the assumption of coarse approximate values for powder by [2]. The main topic of previous works is the explanation of an undesirable effect, which occurs strictly when the solidification step is being initiated. However, the mentioned research efforts do not handle this topic thoroughly. Through experiments with single layers of powder it was observed that under given circumstances the coated powder layer accelerates explosively inside the vacuum chamber [3]. This so-called "powder spreading" effect appears mainly when powder particles are being exposed to the impact of an electron beam at room temperature. The effect exhibits a fundamental restriction on further developments of EBM [2]. With occurrence of this effect in the running process the last positioned powder layer will be destroyed and the layer has to be

recoated. Figure 1 shows the powder spreading effect. The photographs were recorded by use of a high-speed-camera.

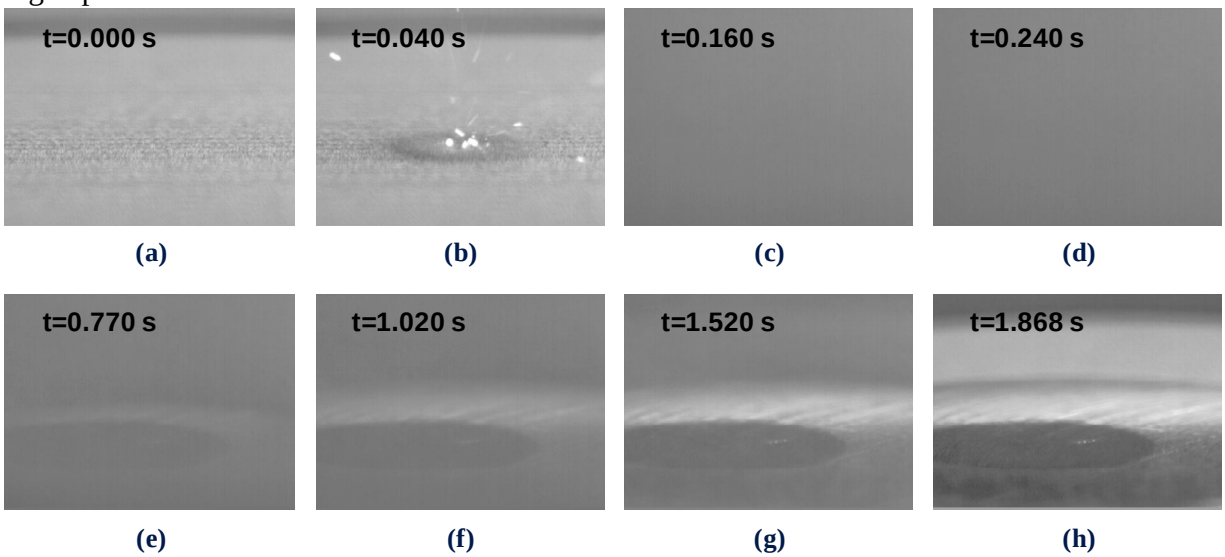

Figure 1: High-speed recording of the powder spreading effect

In Figure 1(a) a powder layer on a base plate with a height of approx. 0.1 mm is shown. The time t = 0.000 s denotes the moment at which the electron beam is being activated with a power of 100 W and first hits the powder layer. Figure 1(b) shows the powder layer at the time t = 0.040 s when the particles with a radius of 10 mm from the beam's point of impact are in motion. Characteristic for that effect is that no large-scale melting of particles occurs [1] and that the beam is not modified in position or power respectively. After additional 0.120 s, Figure 1(c) shows the whole powder layer being accelerated especially in vertical direction. Therefore, only featureless gray boxes can be recognized in Figures 1(c) and 1(d). After t = 0.770 s (cf. Figure 1(e)), the base plate is no longer covered with particles. Instead, the powder is spread inside the vacuum chamber [3].

Various mechanisms for the powder spreading effect have been examined in literature. With the posted approaches *pulse transmission*, *thermodynamics*, *electrostatics* and *electrodynamics* the aim of these explanatory models was to identify the dimension of active forces and so to identify the main contribution to the powder spreading effect. Based on that counteractive measures were designed in order to prevent the powder spreading [3, 4, 5].

Experimental analysis

During interaction of an electron beam with metal a significant fraction of the carried charge is assigned to the irradiated object, the so-called target. If the target is not electrically isolated, the charge is conducted completely to the grounding and no charging effect will take place [6]. According to this, a current through the ground wire can be measured, for example with a digital multimeter. For a more detailed analysis of the powder spreading effect this current i_{Meas} is acquired with a high-resolution measuring board (National Instruments PCI-4070) and synchronized with the recorded pictures of a high-speed-camera (RedLake MotionPro). For this

analysis, the beam current I_B is set to 1 mA and the position of the beam is not deflected. Under equal constraints two different properties for the irradiated surface are chosen. First, the electron beam hits the powder layer and second it hits the blank base plate. So it is possible to acquire the target current under the powder spreading effect as well as the current for the blank surface of compact material (cf. Figure 2). The solid line in Figure 2 shows the target current while hitting the blank base plate. As shown there is an almost constant target current of 0.69 mA, which decreases marginally after 1.1 s and shows higher fluctuation. Compared to that, the dashed line in Figure 2 shows the target current while hitting the powder layer. It is shown that this measured current has a distinctive volatility. After reaching the upper bound of approx. 0.67 mA, the graph declines to approx. 0.09 mA. Apart from small fluctuations, the current rises again after 0.4 s almost monotonically until the end of the measuring period after 2 s.

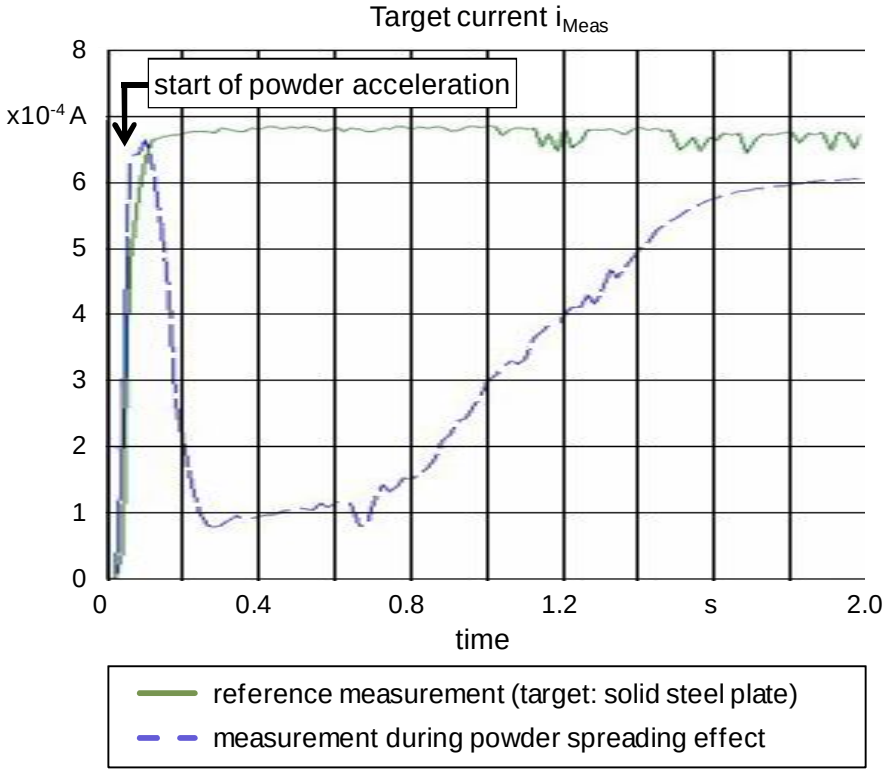

Figure 2: Measurement of target current during powder spreading effect (blue dashed line)

The high-speed-recordings during the powder spreading effect (cf. Figure 1) and the measured currents (cf. Figure 2) were taken concurrently. The frame rate was set to 1000 pictures per second. As it can be seen at time t = 0.240 s rather a powder cloud than a layer can be recognized, i. e. the intensity of the powder spreading effect is on its maximum degree. At the same time the target current is minimal. Thus, it is obvious that the electron beam emits most of its charge by collision with the moving powder particles above the base plate. Only a reduced fraction of the inserted charge can be measured in the ground wire. The further pictures between t = 0.770 s and t = 1.868 s show, that the powder cloud decreases constantly in its intensity and thus, a greater amount of current flows into the base plate and into the ground wire. This monitoring correlates with the measured target current. The value of that current increases steadily up to $i_{Meas} > 0.6$ mA.

Modeling

An important observation through the above mentioned experiment is the 40 ms time-offset between the first contact of beam electrons with the powder surface and the start of powder acceleration (cf. Figure 2). During this lag the powder particles are being charged negatively by the electron beam [6]. The particles' amount of negative charge is crucial to the irradiated material's electrical properties, e. g. electrical conductivity. Furthermore, the charge of the particles depends on the electrical isolation between the particles and the surface of the base plate [7]. However, it seems to be a proper description to split the powder spreading effect into a charge sequence and a discharge sequence (see Figure 3).

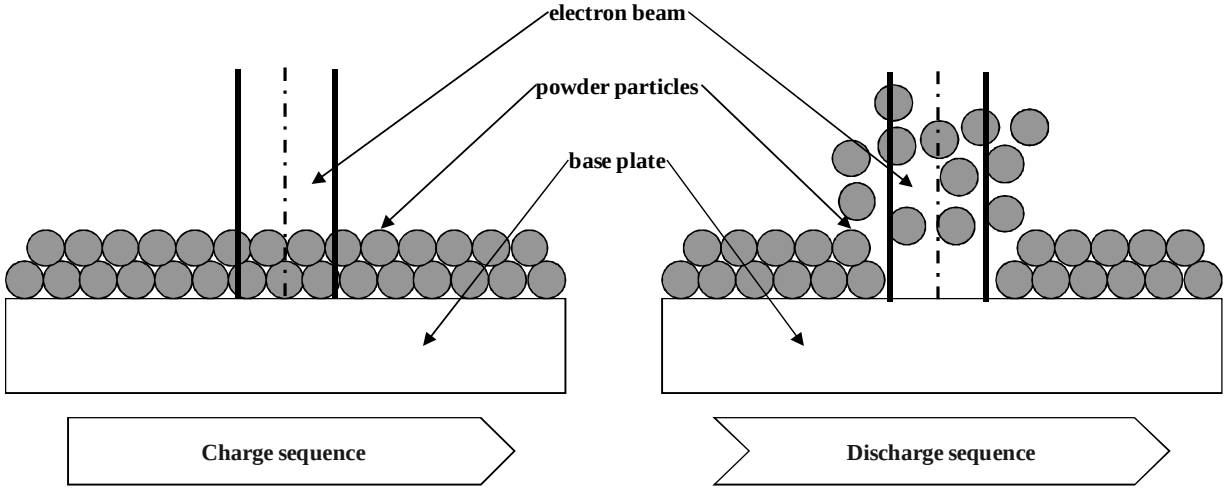

Figure 3: Time-sequences of the powder spreading effect

The charge sequence lasts as long as the electron beam hits the powder and the single particles do not accelerate. With the upcoming spreading effect, the powder is no more under the pressure of the electron beam and thus only the discharge sequence is valid. In the following paragraph, the procedure in the individual sequences will be investigated. An equivalent circuit diagram for the particularly relevant charge sequence will be introduced.

Charge sequence

Due to extremely small contact areas between the single particles, metal powder generally has a considerably high electrical resistance [2]. This value is increased even more at the intersection between powder layer and base plate. This is mostly due to the base plate's plain surface as there is only an exceptionally small contact area between the powder and the base plate [3]. This leads to the effect that the inserted charge cannot flow completely off through the grounded base plate and so it partially remains within the powder layer. Because of this, the powder layer can be assumed as a parallel electrical connection between a resistor and a capacitor [8]. Figure 4 shows the idealized equivalent circuit diagram for the system *electron beam/powder/base plate*.

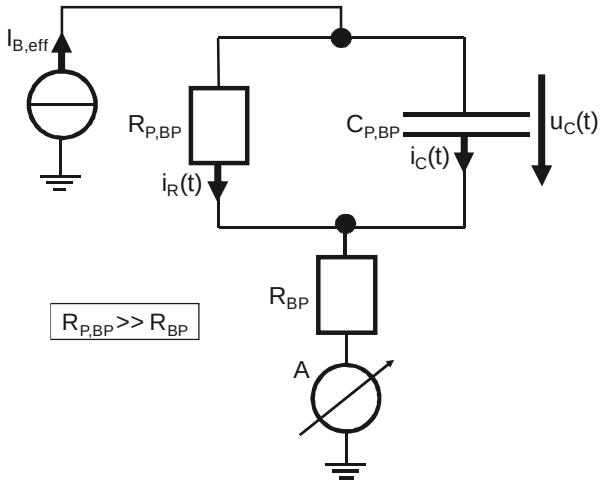

Figure 4: Equivalent circuit diagram for the system electron beam/powder/base plate during the charge sequence

The amount of beam current is given by I_B. Under consideration of the reflected fraction of charge carriers on the surface, the current $I_{B,eff}$ is inserted into the system. The above mentioned parallel connection of $R_{P,BP}$ and $C_{P,BP}$ is in series with the base plate's resistor R_{BP}. The beam current first has to flow through the powder and after that through the base plate to the ground wire. The capacity $C_{P,BP}$ is considered as a parallel-plate capacitor. The powder serves as the negatively charged plate while the base plate serves as the positively charged plate. As mentioned above, the electrical resistance of the powder and its transition to the base plate $R_{P,BP}$ is significantly higher than the resistance of the base plate R_{BP} [2].

Due to the electrostatic interaction between a powder particle of the charge Q_P with other components of the system *electron beam*/*powder*/*base plate* it is exposed to different force influences by the law of electrostatic attraction [9]. First of all the force of repulsion has to be calculated, which a certain powder particle experiences through its interaction with a multitude of further equally charged particles in the powder layer. The force of repulsion $F_{P,P}$ consists of many separate components as expressed in the following equation:

$$F_{P,P}(t) = \frac{1}{4 \cdot \pi \cdot \varepsilon_0} \cdot \sum_{i=1}^{n_P - 1} \frac{Q_P^2(t)}{r_i^2} \tag{1}$$

In eq. (1), the dielectric constant is denoted by ε_0 with a value of $8.854 \cdot 10^{-12}$ C/Vm [9]. The distance between the considered powder particle and an arbitrary further particle i is denoted by r_i. By the following eq. (2), the electrostatic force of repulsion between the electron beam and an also negatively charged powder particle i with the distance to the beam axis $r_{B,i}$ can be caluclated:

$$F_{B,P}(t) = \frac{1}{4 \cdot \pi \cdot \varepsilon_0} \cdot \frac{Q_B \cdot Q_P(t)}{r_{B,i}^2} \tag{2}$$

In eq. (2), the variable Q_B can also be expressed by the following definition:

$$Q_B = \int I_B dt \tag{3}$$

Regardless of the two above mentioned forces of repulsion also a force of attraction arises. This force holds during the charge sequence between the base plate as the positively charged capacitor plate and the powder as the negatively charged capacitor plate. The value of this force of attraction $F_{BP,P}$ is being calculated as follows:

$$F_{BP,P}(t) = -\frac{1}{4 \cdot \pi \cdot \varepsilon_0} \cdot \frac{Q_C \cdot Q_P(t)}{r_{BP,i}^2} \tag{4}$$

The charge of a capacitor's oppositional electrodes has different signs and is of identical value [10]. Thus in eq. (4), the value of Q_C equates the negative charge of the powder as well as the positive charge of the base plate. The distance between an arbitrary particle i of the powder layer and the center of the base plate is denoted by $r_{BP,i}$.

Additional to the mentioned electrostatic interdependencies, a mechanical force interacts between the powder particles in the area of impact. The force takes effect due to the pulse transmission of the moving beam electrons. According to [5], the force has the potential to accelerate powder particles which are hit by the beam and thus overcome the acting force of friction.

The impelling force $F_{e,P}$ can be estimated in consideration of the velocity of the beam electrons v_B as follows [11]:

$$F_{e,P} = m_o \cdot v_B \cdot \frac{I_B}{q} = m_o \cdot c_0 \cdot \sqrt{1 - \frac{1}{\left(1 + \frac{q \cdot U_A}{m_0 \cdot c_0^2}\right)^2}} \cdot \frac{I_B}{q} \tag{5}$$

In eq. (5) the electron mass is denoted by m_0, the electron charge by q. The velocity of light is labeled as c_0. The acting force is assumed to be equally distributed on a circular area of impact A_{imp} with diameter d_{imp} where the beam interacts with the powder. The electron impelling pressure $p_{e,P}$ on the irradiated powder particles can be estimated as follows:

$$p_{e,P} = \frac{F_{e,P}}{A_{imp}} = \frac{4 \cdot I_B \cdot m_o \cdot c_0}{q \cdot d_{imp}^2 \cdot \pi} \cdot \sqrt{1 - \frac{1}{\left(1 + \frac{q \cdot U_A}{m_0 \cdot c_0^2}\right)^2}} \tag{6}$$

As denoted in eq. (1), (2) and (4), the electrostatic forces of repulsion and attraction respectively influence an arbitrary powder particle during the charge sequence. Furthermore, there is an electron impelling force in the area of impact, see eq. (6). Hence, a superposition which leads to a maximum amount of force on the powder particles arises in the area of impact. From that position the layer starts to spread. This assumption is documented by the analysis of high-speed-recordings (cf. Figure 2). It is distinguishable that the powder particles begin to spread initially from the center of the beam in radial direction. Additionally, the particles are also accelerated in vertical direction. This indicates that the powder layer is not hit by the beam directly and the equivalent circuit diagram (cf. Figure 4) for the charge sequence is not valid any more.

Discharge sequence

The discharge sequence during the powder spreading effect is distinguished by the fact that the powder on top of the base plate is moving and no more powder is resting on the base plate. The powder particles accelerate in vertical as well as in radial direction (see Figure 2). As already mentioned, the accelerated powder particles collide with the beam electrons and rest beyond the base plate.

Thus, the electron beam no longer impacts the powder layer, but couples its energy or charge respectively into the grounded base plate. As it will be shown in the following paragraph, it is much more complicated to depict an equivalent circuit diagram for the discharge sequence than for the charge sequence. Additionally, during the discharge sequence the powder spreading effect has already started and thus, adequate counter measures related to the charge sequence need to be considered. As common to a capacitors' discharge sequence, the oppositely charged electrodes equalize. Due to the effect of spreading particles of the system *electron beam*/*powder*/*base plate*, the negatively charged electrode releases its charge. The amount of Q_C is decreasing mainly through this effect. The beam electrons which are inserted into the base plate in spite of their collision with the spread particle, cause a direct charge sink to ground due to $R_{P,BP} >> R_{BP}$. The beam electrons compensate the positively charged base plate, respectively. As a result, no more charging of the residual powder layer takes place during the discharge sequence. The value of Q_P is thus completely determined by the charge sequence.

Since a current can be measured during powder spreading, it indicates that the electron beam hits the base plate in spite of the emerging powder cloud (see Figure 2). Compulsory, this leads to a charge equalization of the base plate which had been positively charged during the charge sequence. In conjunction with the high electrical resistance $R_{P,BP}$ it follows that the powder particles spread before giving their negative charge completely into the base plate. From this it follows that the mentioned electrostatic forces are valid during the discharge sequence as well. Since the powder particles are in motion, the electron beam cannot apply a force on the powder layer and so the electron beam pressure force can be neglected.

During the discharge sequence another mechanism, namely the Lorentz force influences the powder spreading. The fundamental condition for that is that a negatively charged powder particle is accelerated to the velocity v by the above mentioned force. When crossing the magnetic field induced by the electron beam at flux density B a Lorentz force F_L on the powder particle is being generated [9]. The force causes a vertical acceleration, as noted in eq. (7).

$$F_L = Q_P \cdot (v \times B) = Q_P \cdot \left(v \times \left(\mu_0 \cdot \frac{I_B}{2 \cdot \pi \cdot R} \right) \right) \tag{7}$$

In eq. (7), the diameter of a current-carrying conductor of equal power to the electron beam is denoted by R. The magnetic flux density is denoted by μ_0 which is equal to $4 \cdot \pi \cdot 10^{-7}$ Vs/Am.

Conclusion from the model

The quantitative prediction of process parameters is very complex. Since for proper determination the total number of powder particles and their respective properties, such as geometry, particle size distribution and electrical properties have to be considered within the calculation. Hence, a considerable computing effort would result. Therefore, the presented analytical model is used in order to predict the qualitative behavior of the powder spreading effect.

As a result of the previously mentioned modeling, qualitative estimations for possible input coefficients are given (cf. eq. (1), (2) and (4)). An important aspect of previous sections is the time-discretization of the powder spreading effect during the charge as well as during the discharge sequence. For a proper understanding, the distinction between causative and acting forces during the persistent powder spreading effect is important. The focus of consideration is the prevention of the powder spreading effect. Since the charge sequence is terminated with the upcoming spreading effect, the following explanations focus on the acting forces and pressure components (see Table 1).

Value	**Description**	**Eq.**	**Charge sequence**	**Discharge sequence**	**Basic parameter**
$F_{P,P}$	Electrostatic force (particle/particle)	(1)	x	x	$R_{P,BP}$, $C_{P,BP}$, I_B, r_i
$F_{B,P}$	Electrostatic force (beam/particle)	(2)	x	x	$R_{P,BP}$, $C_{P,BP}$, I_B, U_A, $r_{B,i}$
$F_{BP,P}$	Electrostatic force (base plate/particle)	(4)	x	x	$R_{P,BP}$, $C_{P,BP}$, I_B, $r_{BP,i}$
$p_{e,P}$	Electron impelling pressure	(6)	x		I_B, U_A, d_{imp}
F_L	Lorentz force	(7)		x	-

Table 1: Analysis of the action of force and its causative basic parameters

In this context, “basic parameter” denotes the variables, which have direct or indirect impact on the mentioned equations of force and pressure components, respectively. It is notable that the electric resistance $R_{P,BP}$ and capacitance $C_{P,BP}$ of the system *powder*/*base plate* as well as the beam current I_B appear especially common. For the sake of clarity the basic parameter $I_{B,eff}$ is reduced to I_B, since a change of I_B under equal preconditions leads to a direct variation of $I_{B,eff}$. Furthermore, the acceleration voltage U_A and the beam spot diameter d_{imp} are relevant. It is notable, that table 1 contains further basic parameters. First, the value r_i concerns the distance between the powder particle under consideration and a further particle i. Second, the distance between a powder particle i to the beam axis is denoted by $r_{B,i}$. Third, the distance between an arbitrary powder particle i to the center of the base plate is described by $r_{BP,i}$. These values are required in order to estimate the acting forces on a representative powder particle in eq. (1), (2) and (4). Hence, they do not constitute a layer property and thus, can be neglected for further evaluations. Since the considerations for prevention of the powder spreading effect are restricted

to force and pressure effects during the charge sequence, the basic parameters of the Lorentz force are disregarded, too.

Experimental validation

In order to achieve a matching between the mathematical-physical modeling of the powder spreading effect and real conditions, an experimental validation has to be arranged. According to table 1, the parameters "beam current" I_B, "accelerating voltage" U_A, "beam spot diameter" d_{imp}, "shape of the powder particles" and the "preheating temperature" T_P are relevant to the occurrence of the powder spreading effect. Some of the basic parameters (I_B, U_A, d_{imp}) are directly reflected in these factors. In terms of $R_{P,BP}$ and $C_{P,BP}$, these influences are being considered by the preheating temperature T_P as well as by the particle shape. Both parameters have an impact on the resulting values of $R_{P,BP}$ and $C_{P,BP}$ [2]. The focus of experimental design is to evaluate impacts on the undesirable powder spreading effect. For this purpose, the chosen input parameters I_B, U_A, d_{imp}, T_P as well as the shape of particles are modified in two steps (cf. Figure 5). The layer thickness is set to 0.1 mm and the particle diameter fraction is 10 µm to 60 µm for both types of powder.

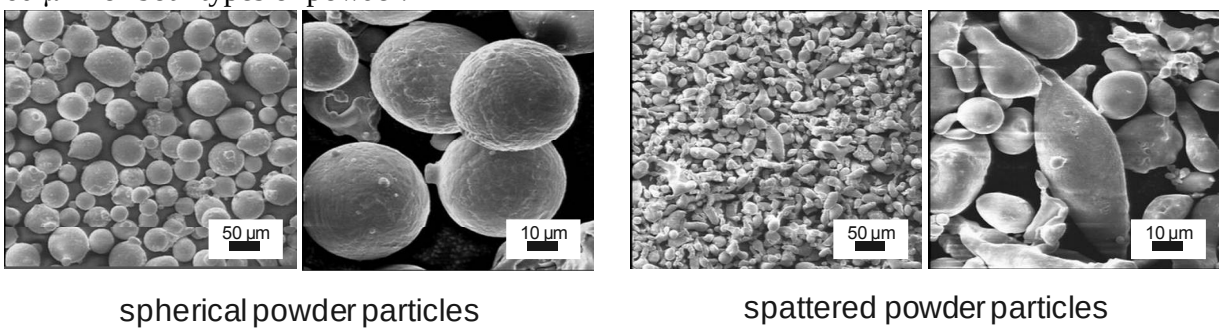

Figure 5: Scanning electron microscope recordings of different powder particles shapes

When all combinations are handled in terms of a full-factorial experimental design, a total number of $2^5 = 32$ parameter settings result. The focus of the scientific experiments is to hold the beam current on the specified value over a fixed period of ten seconds for every single test. However, when powder spreading occurs, the beam is deactivated immediately. In case the powder spreading effect has not taken place within the predefined period, the single test is completed and the powder is deemed not to be spread. In order to limit complexity of the experiments, the electron beam is neither altered in position nor altered in power during the defined period. For all experiments, the beam impacts the powder layer in its center. During preheating of the powder, the strongly defocused beam is moved across the layer in the shape of a circular area. The diameter of the circular area is 80 mm and the figure is defined by 1000 points. The overall area of the circle is being exposed to the beam 500 times within a second. Meanwhile, the beam current is linearly increased at 0.2 mA/s starting from 0 mA. This happens as long as the attached pyrometer indicates the adjusted preheating temperature T_P of the powder layer. The used experimental design gives a review over the chosen settings (cf. Table 2). In order to eliminate unintentional impacts like trends, the order of the single experiments is defined randomly. Since the modification from one material to another involves a considerable effort, the overall experiment is divided into two parts. Within the first part (no. 1 to no. 16) the spattered

powder is examined, whereas in the second part (no. 17 to no. 32) the evaluations are limited to spherical powder. Therefore, the stochastic distribution of experiments is only valid within the particular sections. Besides the experimental design, table 2 shows the results of the single experiments.

Nr.	Shape of particles	T_P [°C]	d_{imp} [mm]	I_B [mA]	U_A [kV]	Powder spreading		Remarks
						Yes	No	
1	spattered	25	0.4	0.5	100		x	
2	spattered	600	0.4	5.0	60		x	
3	spattered	600	0.2	0.5	100		x	
4	spattered	25	0.4	0.5	60		x	
5	spattered	25	0.2	5.0	100	x		
6	spattered	600	0.2	5.0	60		x	
7	spattered	25	0.2	0.5	60	x		
8	spattered	25	0.2	5.0	60	x		
9	spattered	600	0.2	0.5	60		x	
10	spattered	25	0.2	0.5	100	x		
11	spattered	25	0.4	5.0	100	x		
12	spattered	25	0.4	5.0	60	x		
13	spattered	600	0.2	5.0	100		x	
14	spattered	600	0.4	5.0	100		x	
15	spattered	600	0.4	0.5	60		x	
16	spattered	600	0.4	0.5	100		x	
17	spherical	600	0.4	0.5	100	x		During preheating
18	spherical	600	0.2	0.5	60	x		During preheating
19	spherical	25	0.4	0.5	100	x		
20	spherical	25	0.4	5.0	60	x		
21	spherical	25	0.4	0.5	60	x		
22	spherical	25	0.2	0.5	100	x		
23	spherical	600	0.2	0.5	100	x		During preheating
24	spherical	600	0.4	5.0	100	x		During preheating
25	spherical	600	0.2	5.0	60	x		During preheating
26	spherical	25	0.2	5.0	100	x		
27	spherical	600	0.4	5.0	60	x		During preheating
28	spherical	25	0.2	0.5	60	x		
29	spherical	25	0.4	5.0	100	x		
30	spherical	600	0.4	0.5	60	x		During preheating
31	spherical	600	0.2	5.0	100	x		During preheating
32	spherical	25	0.2	5.0	60	x		

Table 2: Experimental design and results for the powder spreading effect

It is noticeable that powder spreading of a layer of spherical particles can neither be avoided at room temperature nor at preheating temperature of 600 °C. Rather it is monitored that the powder starts spreading even during the preheating step. Hence, the experimental validation of the chosen beam properties is not possible. In contrast, the undesirable phenomenon never appears with spattered powder and a preheating temperature of 600 °C. As a further result, it is proven that an increasing defocusing of the electron beam leads to a positive effect. By increasing the beam spot diameter to a value of 0.4 mm, the powder spreading effect can be avoided in six single experiments. On the contrary, with a beam spot diameter of 0.2 mm this only holds true for four single experiments. Since the spreading effect can be avoided six times with $I_B = 0.5$ mA and only four times with $I_B = 5$ mA, the reduction of beam current is significant. However, the

influence of the accelerating voltage is less relevant. With both values of 60 kV and 100 kV respectively, spreading takes place three times each.

Conclusion

The presented work relates to the increase of process stability for Electron Beam Melting (EBM). Up to date, the powder spreading phenomenon constitutes a considerable deficiency as the top layer of particles is being pushed away from the building plate. Hence, the deposition of another layer needs to be performed or the building job must be aborted respectively. Therefore, a modeling approach is being formulated concerning the examination of electrostatic, impelling electron and Lorentz forces. As a result, the respective influencing parameters were determined and thus, used for experimental validation with the EBM equipment. It was detected, that the given equations sufficiently correlate with the conducted experiments.

As pointed out in the previous section, the experimental results exhibit main influencing factors on the spreading effect. In this context, it is particularly notable, that the powder layer is able to be exposed to the electron beam at room temperature without the appearance of spreading when a beam spot diameter of 0.4 mm is being applied. Thus, the process step “preheating the powder layer” as it is state of the art in EBM can be neglected and a considerable saving of time can be achieved. Furthermore, the efforts in terms of the removal of unmelted powder can be significantly reduced as the formation of sinter bonds is eliminated.

The experiments also indicate that the powder spreading effect occurs permanently whenever spherical powder is being applied to the process. In reference to the previous modeling, the shape of the particles has a significant influence on the electrical resistance $R_{P,BP}$ as well as on the capacity $C_{P,BP}$ respectively. According to [3], spherical powder particles lead to an increase in electrical conductivity due to the fact that more and greater contact areas exist among the particles as well as between the particles and the base plate. However, further research needs to be conducted in terms of the determination of the capacity of the system *powder*/*base plate* as a function of the particle shape and the size distribution.

References

[1] Meindl, M.: Beitrag zur Entwicklung generativer Fertigungsverfahren für das Rapid Manufacturing. Diss. Technische Universitaet Muenchen (2004). Muenchen: Utz 2005.

[2] Sigl, M.: Entwicklung von Rapid-Technologien am Beispiel des Elektronenstrahlsinterns. Diss. Technische Universitaet Muenchen (2008). Muenchen: Utz 2008.

[3] Sigl, M.; Zäh, M. F.; Lutzmann, S.: Transient Physical Effects in Electron Beam Sintering. In: Bourell, D. L. (Eds.): Solid Freeform Fabrication Symposium 2006.

[4] Kahnert, M.; Lutzmann, S.; Zäh, M. F.: Layer Formations in Electron Beam Sintering. In: Bourell, D. L. (Eds.): Solid Freeform Fabrication Symposium 2007.

[5] Qi, H. B.; Yan, Y. N.; Lin, F.; He, W.: Direct metal part forming of 316L stainless steel powder by electron beam selective melting. (Eds.): Proceedings of the Institution of Mechanical Engineers -- Part B -- Engineering Manufacture 2006, pp. 1845–1853.

[6] Ardenne, M. v.: Tabellen zur angewandten Physik: Elektronenphysik, Ionenphysik, Vakuumphysik, Kernphysik, medizinische Elektronik, Hilfsgebiete. Berlin: Dt. Verl. der Wiss. 1962.

[7] Iinoya, K.; Gotoh, K.; Higashitani, K.: Powder Technology Handbook. New York (USA): Marcel Dekker 1991.

[8] Kories, R.; Schmidt-Walter, H.: Electrical Engineering – A Pocket Reference. Norwood (USA): Artech House Publishers 2007.

[9] Resnick, R.; Halliday, D.; Krane K. S.: Physics. 5th Ed. New York (USA): John Wiley and Sons 2001.

[10] Flegel, G.; Birnstiel, K.; Nerreter, W.: Elektrotechnik für Maschinenbau und Mechatronik. 8th Ed. Muenchen: Hanser 2004.

[11] Crawford, C. K.: Electron Beam Machining: Introduction to Electron Beam Technology. New York (USA): John Wiley and Sons 1962.